Non-homologous end joining minimizes errors by coordinating DNA processing with ligation

Benjamin M. Stinson[1], Andrew T. Moreno[1], Johannes C. Walter[1,2,*] & Joseph J. Loparo[1,*]

[1] Department of Biological Chemistry and Molecular Pharmacology, Harvard Medical School, Boston, MA 02115, USA
[2] Howard Hughes Medical Institute, Boston, MA 02115, USA
* Correspondence: johannes_walter@hms.harvard.edu (J.C.W.); joseph_loparo@hms.harvard.edu (J.J.L)

Genome stability requires efficient and faithful repair of DNA double-strand breaks (DSBs). The predominant DSB repair pathway in human cells is non-homologous end-joining (NHEJ), which directly ligates DNA ends[1–5]. Broken DNA ends at DSBs are chemically diverse, and many are not compatible for direct ligation by the NHEJ-associated DNA Ligase IV (Lig4). To solve this problem, NHEJ end-processing enzymes including polymerases and nucleases modify ends until they are ligatable. How cells regulate end processing to minimize unnecessary genomic alterations[6] during repair of pathological DSBs remains unknown. Using a biochemical system that recapitulates key features of cellular NHEJ, we previously demonstrated that DNA ends are initially tethered at a distance, followed by Lig4-mediated formation of a "short-range synaptic complex" in which DNA ends are closely aligned for ligation[7]. Here, we show that a wide variety of end-processing activities all depend on formation of the short-range complex. Moreover, using real-time single molecule imaging, we find that end processing occurs within the short-range complex. Confining end processing to the Lig4-dependent short-range synaptic complex promotes immediate ligation of compatible ends and ensures that incompatible ends are ligated as soon as they become compatible, thereby minimizing end processing. Our results elucidate how NHEJ exploits end processing to achieve versatility while minimizing errors that cause genome instability.

Keywords: non-homologous end joining, NHEJ, processing

NHEJ is initiated by the ring-shaped Ku70/Ku80 heterodimer (Ku)[8,9], which encircles broken DNA ends and recruits the DNA-dependent protein kinase catalytic subunit (DNA-PKcs)[10]. DNA-PKcs phosphorylates multiple NHEJ factors, including itself, and its kinase activity is required for efficient end joining[11–13]. Ends are ligated by a complex of DNA Ligase IV (Lig4) and XRCC4[14,15], and joining is stimulated by the XRCC4 paralog XLF[16]. End-processing enzymes act in concert with these core factors to allow joining of chemically incompatible ends. Such processing enzymes include DNA polymerases (e.g., pol λ, pol μ)[17–21], nucleases (e.g., Artemis)[22], polynucleotide kinase 3'-phosphatase (PNKP)[23], and tyrosyl-DNA phosphodiesterase 1 (Tdp1)[24], which removes certain 3' adducts[25]. Although end-processing enzymes have the potential to generate mutations—the basis of gene disruption by CRISPR-Cas9 technology—NHEJ appears optimized to maximize fidelity, as compatible ends are directly ligated, and incompatible ends are minimally processed[6]. Prevailing models, which posit that each DNA end is processed independently and stochastically[3,19,26,27], predict a wide variety of junction sequences and do not readily explain the conservative properties of NHEJ. Thus, despite important implications for genome maintenance and editing, how NHEJ limits mistakes while maintaining the capacity for processing remains unknown.

To understand how end processing is regulated, we used cell-free *X. laevis* egg extracts, which join DNA ends in a manner dependent on Ku, DNA-PKcs, Lig4-XRCC4, and XLF[7,28–31]. We generated a series of linear DNA substrates with compatible or incompatible ends (Fig. S1). Compatible ends (i.e., blunt, complementary) were typically ligated without processing (Fig. S1b, #1-3), consistent with cell-based studies[6]. In contrast, incompatible ends underwent a variety of processing events prior to joining, including 5'-phosphorylation, gap-filling, nucleolytic trimming, and 3'-adduct removal (Fig. S1b, #4-10). To identify end-processing enzymes in this cell-free system, we performed immunodepletion and reconstitution experiments. Immunodepletion of both pol λ and pol μ prevented gap-filling (Fig. S2a,b). Consistent with previous reports[32], re-addition of recombinant pol λ but not pol μ restored efficient gap-filling of DNA ends with paired primer termini (Fig. S2a); conversely, pol μ but not pol λ supported gap-filling with unpaired primer termini (Fig. S2b). Tdp1 was required for removal of a 3'-adduct (Fig. S2c), and PNKP was essential for phosphorylation of 5'-hydroxyl ends prior to joining (Fig. S2d). 5' flaps were removed by a nuclease prior to joining (Fig. S1, #9). However, immunodepletion of Artemis, a nuclease implicated in NHEJ[33], had no effect on joining of these ends (Fig. S2f), suggesting involvement of an unidentified nuclease. PNKP, pol λ, pol μ, and Tdp1 were not required for joining of compatible ends, indicating that these enzymes are dispensable for the core NHEJ reaction (Fig. S2e). Thus, as seen in vivo[6], *X. laevis* egg extracts support efficient end processing but employ this mechanism only when necessary.

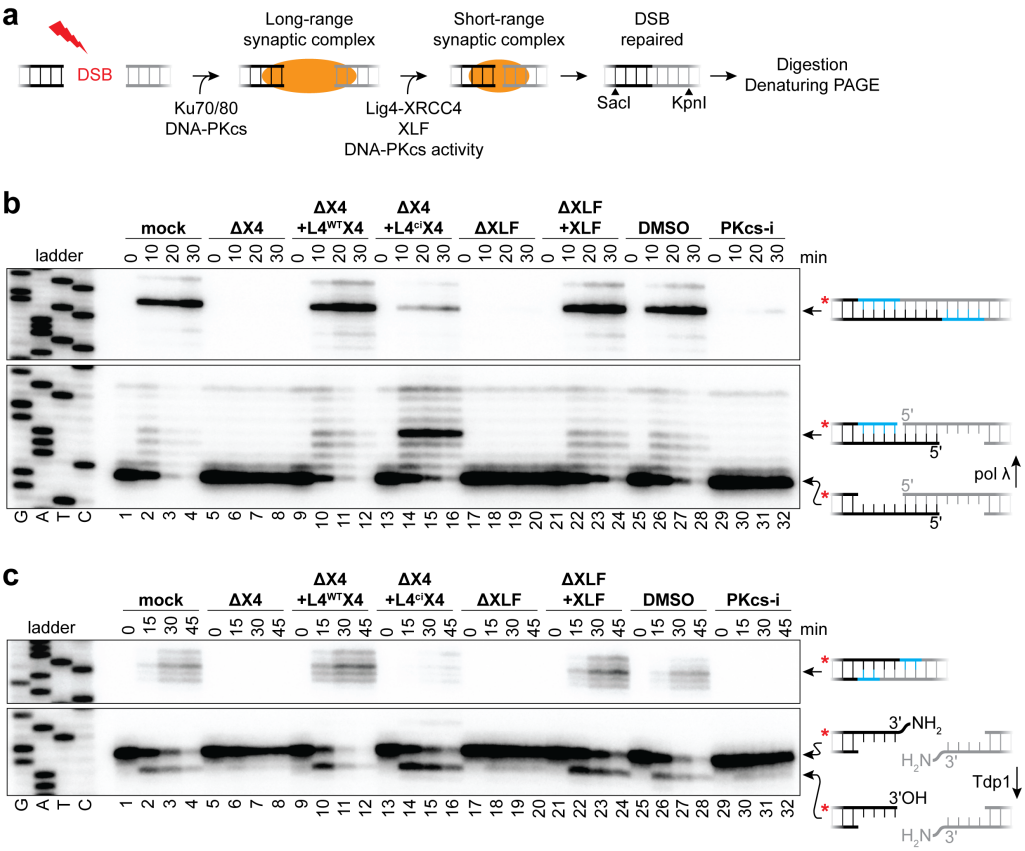

Figure 1: Disruption of short-range synapsis inhibits end processing by pol λ and Tdp1. a, Model of two-stage DNA end synapsis during NHEJ[7]. Triangles indicate restriction sites for digestion and analysis of NHEJ joints by denaturing PAGE. **b**,**c**, Radiolabeled linear DNA molecules with the depicted ends were added to the indicated egg extracts, and reaction samples were stopped at the indicated time points. DNA was extracted, digested, and analyzed by denaturing PAGE and autoradiography. Lower panels, un-joined DNA ends; upper panels, joined DNA ends. Single-molecule experiments verified that XRCC4 immunodepletion, XLF immunodepletion, and DNA-PKcs inhibition blocked short-range synapsis of the ends in **b** (Fig. S4a), as reported previously for blunt ends[7]. Red asterisk indicates radiolabeled strand; both strands are processed and ligated, but this need not occur simultaneously. X4, XRCC4; $L4^{WT}$ and $L4^{ci}$, wild-type and catalytically-inactive Lig4, respectively.

We reasoned that end processing might be coordinated with synapsis, which aligns DNA ends for ligation. Previously, we described a two-stage model of synapsis (Fig. 1a)[7]: initially, Ku and DNA-PKcs form a "long-range" synaptic complex in which DNA ends are held >100 Å apart; subsequently, DNA-PKcs kinase activity, XLF, and Lig4-XRCC4 convert the long-range complex into a "short-range" complex in which ends are held close together in a ligation-competent state. Based on this model, we hypothesized that end processing occurs only in the Lig4-dependent short-range synaptic complex. Such a mechanism would promote immediate ligation of compatible ends and ensure that incompatible ends undergo ligation as soon they become compatible, thereby minimizing processing.

A prediction of this hypothesis is that disruptions of short-range synapsis should block end processing. To test this idea, we used three independent means—Lig4-XRCC4 immunodepletion, XLF immunodepletion, or DNA-PKcs inhibition—to block short-range synapsis and asked whether end processing was inhibited. Immunodepletion of XRCC4 (Fig. S3a), which also depletes Lig4[7], inhibited gap filling by pol λ (Fig. 1b, lanes 1-8). Gap filling was restored by recombinant wild-type or catalytically-inactive Lig4-XRCC4 (Fig. 1b, lanes 9-16), both of which support short-range synapsis[7]. Catalytically-inactive Lig4-XRCC4 supported a low level of joining (Fig. 1b, compare lanes 13-16 to lanes 5-8), likely because it promotes generation of compatible ends that can be joined by residual endogenous Lig4-XRCC4 or another ligase[34]. Like Lig4-XRCC4, XLF and DNA-PKcs kinase activity were required for gap filling (Fig. 1b, lanes 17-32; Fig. S3a). We next asked whether short-range synapsis is generally required for processing. Strikingly, 3'-adduct removal by Tdp1 (Fig. 1c), gap-filling by pol μ (Fig. S3b), 5'-hydroxyl phosphorylation by PNKP (Fig. S3c), and nucleolytic flap removal (Fig. S3d) all depended on Lig4-XRCC4, XLF, and DNA-PKcs kinase activity. Thus, three independent perturbations of short-range synapsis substantially inhibited every processing activity measured, strongly suggesting that end processing depends on short-range synapsis.

Our results are consistent with the idea that end processing occurs within the short-range complex. However, they cannot exclude a model[35] in which incompatible DNA ends dissociate before undergoing processing, followed by subsequent synapsis and ligation attempts. To distinguish between these models, we performed single-molecule FRET analysis to simultaneously monitor DNA-end synapsis and processing in real time. We attached a ~3 kb linear DNA molecule with 5' overhangs to a passivated glass coverslip in a microfluidic channel (Fig. 2a). To monitor short-range synapsis using FRET, we placed a donor fluorophore near one DNA end and an acceptor fluorophore near the other end[7]. The extract was supplemented with dUTP labeled with the dark quencher BHQ-10 ($dUTP^Q$; Fig. S4b) so that $dUTP^Q$ incorporation opposite a templating adenosine would quench donor fluorescence (Fig. 2a). Ensemble experiments demonstrated that $dUTP^Q$ was efficiently incorporated during joining of these ends (Fig. S4c lanes 5-8). Figure 2b shows a representative single-molecule fluorescence trajectory during joining in the presence of $dUTP^Q$. After addition of extract, we observed a transition from a low-FRET state to a high-FRET state, indicating short-range synapsis had occurred,

followed by quenching in the high-FRET state. Subsequent quencher "blinking" (Fig. S5) caused periodic return of donor fluorescence (Fig. 2b), allowing us to unambiguously identify bona fide quenching events and exclude donor photobleaching. Importantly, the vast majority (~80%) of quenching events occurred in the high-FRET state ($FRET_E \approx 0.5$; Fig. 2c, blue) even though the low-FRET state was much more abundant overall ($FRET_E \approx 0$; Fig. 2d, blue). Inclusion of dTTP instead of $dUTP^Q$ revealed a background frequency of low-FRET quenching events (Fig. 2c, red) similar to that observed when $dUTP^Q$ was present (Fig. 2c, blue), suggesting that $dUTP^Q$ incorporation does not occur to any detectable extent in the low-FRET state. Changing the template base from adenine to thymine, inclusion of dTTP instead of $dUTP^Q$, combined immunodepletion of pol λ and pol μ, or inhibition of DNA-PKcs all suppressed $dUTP^Q$ incorporation (Fig. S4c, lanes 9-28) and high-FRET quenching events (Fig. 2c, yellow; Fig. S4e,f). We conclude that pol λ activity is tightly coupled to the short-range synaptic complex.

We next asked whether Tdp1 also acts in the short-range synaptic complex. We generated a DNA substrate with a Tdp1-labile, donor-labeled 3' adduct on one end and an acceptor fluorophore in the duplex region of the other end, thereby allowing observation of short-range synapsis via FRET and Tdp1 activity via loss of donor signal (Fig. 3a). Ensemble experiments verified that the fluorescent 3' adduct was efficiently removed prior to joining (Fig. S7a, lanes 1-4). To prevent competition from resection in single-molecule experiments, we depleted extracts of Mre11, which did not affect end processing or joining (Fig. S7a, lanes 5-8). We frequently observed a transition from a low-FRET state to a high-FRET state followed by a loss of donor signal (e.g., Figure 3b). The majority (~60%) of donor loss events occurred in the high-FRET state (Fig. 3c, blue) despite its low overall abundance (~20% of all frames; Fig. 3d, blue). Thus, donor loss occurred ~5-fold more quickly in the high-FRET state (Fig. 3e, solid blue vs. dashed blue). Tdp1 immunodepletion greatly reduced the frequency of donor loss events from both low- and high-FRET states (Fig. 3c, red), and this reduction was rescued upon addition of recombinant Tdp1 (Fig. 3c, yellow), indicating that Tdp1 and not photobleaching was responsible for the vast majority of detected donor loss events. The occasional donor loss events from the low-FRET state likely correspond to Tdp1 activity on transiently unprotected ends (see below). In summary,

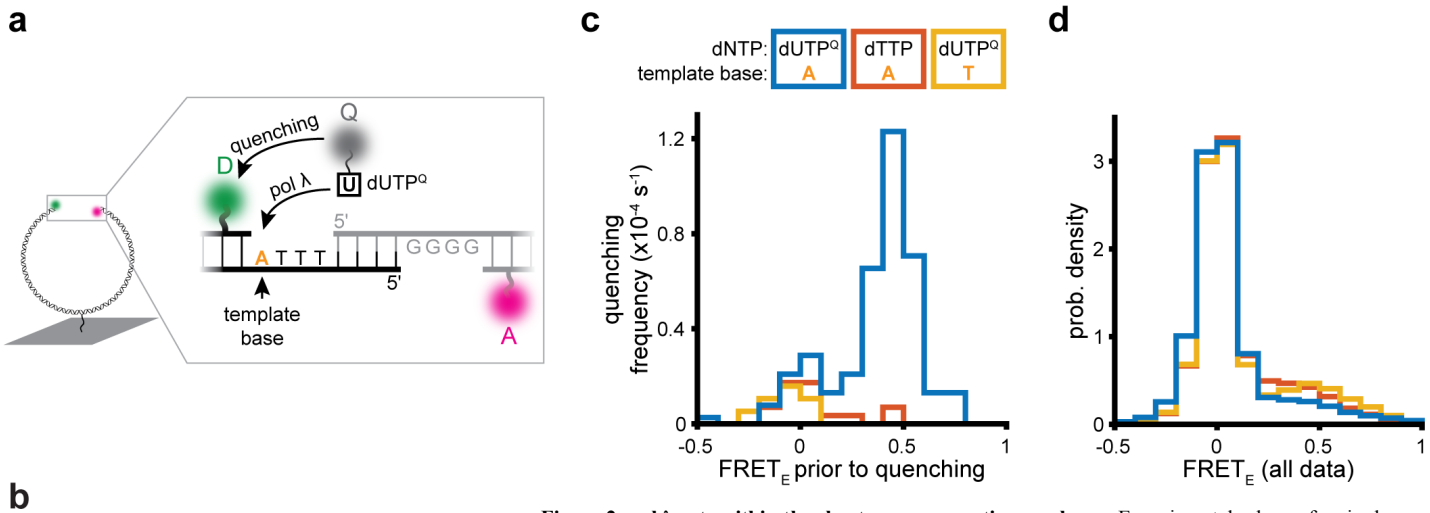

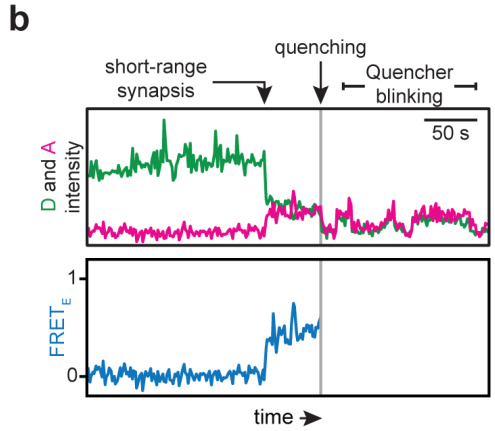

Figure 2: pol λ acts within the short-range synaptic complex. a, Experimental scheme for single-molecule assay of DNA-end synapsis and polymerase activity. A linear DNA molecule fluorescently labeled at both ends was attached to a glass coverslip within a microfluidic chamber, and extracts supplemented with dATP, dCTP, dGTP and $dUTP^Q$ were introduced to the chamber. D, Cy3 donor fluorophore; A, Cy5 acceptor fluorophore; Q, BHQ10 quencher. Addition of fluorophores did not inhibit joining (Fig. S4d). Fluorophore positions are not to scale—Cy3 and Cy5 were placed five bases from the 3' ends (Table S1). **b**, Example trajectory. The Cy3 donor fluorophore was excited and donor emission (green) and Cy5 acceptor emission (magenta) were recorded (upper panel) and used to calculate FRET efficiency (blue, lower panel). FRET transitions, identified by anti-correlated changes in donor and acceptor intensity, marked short-range synapsis. Quenching was identified as a sharp decrease in donor intensity below a set threshold without a corresponding increase in acceptor intensity, and was characteristically followed by blinking (see Fig. S5). **c**, Frequency of quenching events as a function of FRET efficiency immediately prior to quenching under the indicated conditions. Blue, extracts supplemented with $dUTP^Q$, adenine DNA template base (Fig. 2a) substrate (n = 145 events from 9 independent experiments); red, extracts supplemented with dTTP, adenine DNA template base substrate (n = 16 events from 6 independent experiments); yellow, extracts supplemented with $dUTP^Q$, thymine DNA template base (n = 8 events from 6 independent experiments). Quenching frequency was calculated by dividing the number of quenching events by the total observation time prior to censoring by quenching, donor or acceptor photobleaching, or end of experiment. Observation times were identical for all experiments (900 s). See Fig. S6a for kinetic analysis and histograms represented as probability density. **d**, Histogram of the FRET efficiency of all frames for all molecules prior to censoring. Colors as in **c**.

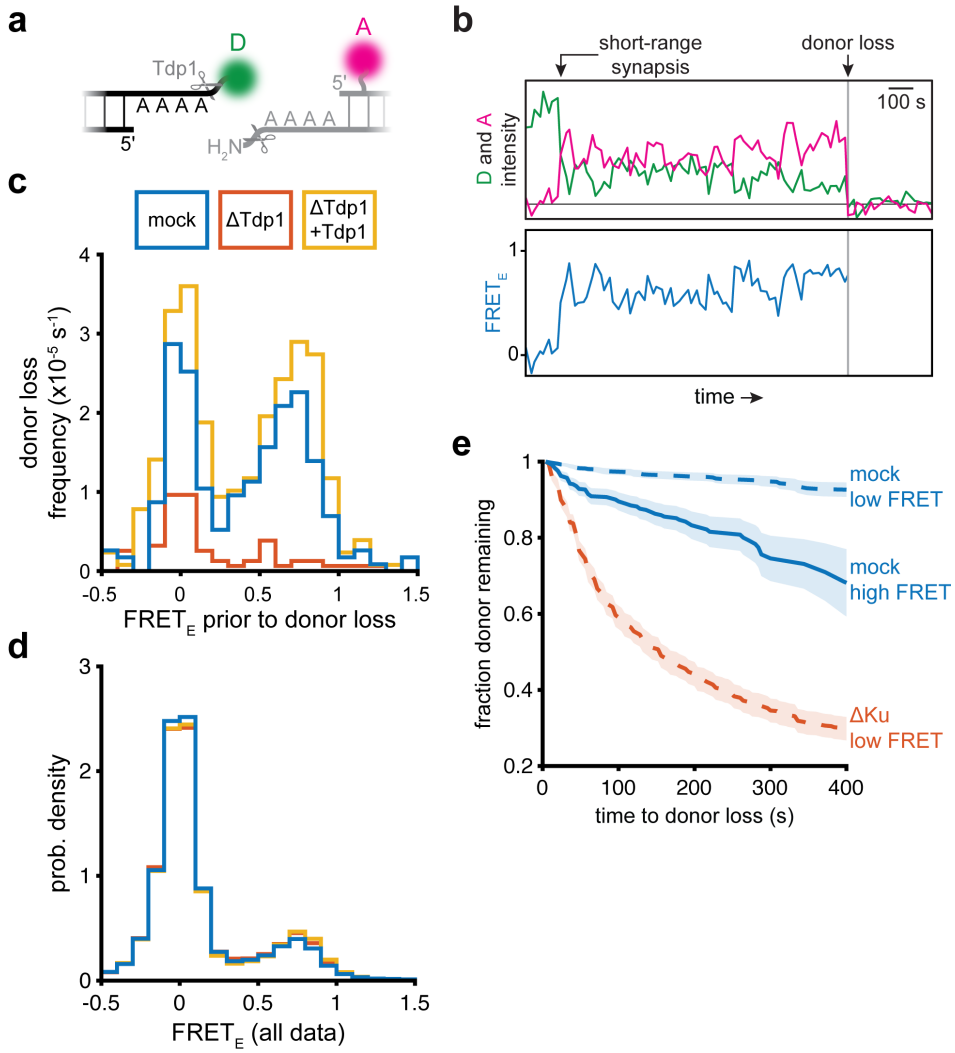

Figure 3: Short-range synapsis accelerates Tdp1 activity. a, Experimental scheme for single-molecule assay of Tdp1 activity and DNA-end synapsis. Linear DNA was attached to a coverslip in a microfluidic channel as in Fig. 2a. Cy3B was coupled to the 3'-end of the oligonucleotide used to construct the substrate depicted in Fig. 1c (see Fig. S1 #10 for chemical structure). D, Cy3B donor fluorophore; A, ATTO647N acceptor fluorophore. **b**, Example trajectory. The Cy3B donor fluorophore was excited and donor emission (green) and ATTO647N acceptor emission (magenta) were recorded (upper panel) and used to calculate FRET efficiency (blue, lower panel). FRET transitions, identified by anti-correlated changes in donor and acceptor intensity, marked short-range synapsis. Donor loss was identified as a sharp decrease in donor intensity below a set threshold. **c**, Frequency of donor loss events as a function of FRET efficiency immediately prior to donor loss under the indicated conditions. Blue, mock-depleted extracts (n = 222 events from 2 independent experiments); red, Tdp1-depleted extracts (n = 65 events from 2 independent experiments); yellow, Tdp1-depleted extracts supplemented with 40 nM recombinant Tdp1 (n = 339 events from 2 independent experiments). Donor loss frequency was calculated by dividing the number of donor loss events by the total observation time prior to censoring by donor loss, acceptor photobleaching, or end of experiment. Observation times were identical for all experiments (1800 s). See Fig. S8a-c for histograms represented as probability density and kinetic analysis. **d**, Histograms of FRET efficiency of all frames for all molecules prior to censoring. Colors as in **c**. **e**, Donor survival kinetics (Kaplan-Meier estimate) under the indicated conditions. The x-axis indicates dwell time in the high-FRET (solid line) or low-FRET (dashed lines) state prior to donor loss. Blue, donor survival kinetics in mock-depleted extract (n = 76 events, dashed line; 107 events, solid line); red, donor survival kinetics in Ku-depleted extract (n = 687 events); shaded areas, 95% confidence intervals.

in all cases, efficient processing required formation of the short-range complex; in at least two of these—gap filling and adduct removal—end processing occurred preferentially in the high FRET state. Together, the data suggest that processing generally occurs in the short-range complex.

We next addressed how end processing is prevented before formation of the short-range synaptic complex. One possibility is that short-range synapsis is required to recruit end-processing enzymes. To test this idea, we examined binding of end-processing enzymes to DNA ends in the presence or absence of DNA-PKcs inhibitor, which blocks short-range synapsis (Fig. 4a, S9). However, as shown in Fig. 4a, PNKP, pol λ, pol μ, and Tdp1 were each enriched on DSB-containing DNA whether or not the short-range synaptic complex was allowed to form, suggesting that end-processing enzymes are recruited prior to short-range synapsis.

Based on the above results, we postulated that prior to short-range synapsis, core NHEJ factors protect DNA ends from bound processing factors. Indeed, immunodepletion of Ku (Fig. S10a) caused aberrant fill-in of 5' overhang ends without subsequent joining (Fig. 4b, lanes 5-8), consistent with a role for Ku in DNA end protection[36,37]. Re-addition of recombinant Ku restored typical gap-filling and joining (Fig. 4b, lanes 9-12). Importantly, aberrant fill-in occurred even when pol λ and pol μ were immunodepleted (see Fig. 4b legend) in combination with Ku, suggesting a non-NHEJ polymerase fills in 5' overhang ends when Ku is absent (Fig. 4b, lanes 17-20; Fig. S10b). Ku also suppressed aberrant 3'→5' exonuclease activity following 3' adduct removal (Fig. 4c, lanes 5-12). Combined immunodepletion of Ku and Tdp1 (Fig. S10c) prevented both 3'-adduct removal and exonuclease activity (Fig. 4c, lanes 17-20), and addition of recombinant Tdp1 restored these activities (Fig. 4c, lanes 21-24). Thus, Tdp1 can access DNA ends in the absence of Ku, but ends are protected in the presence of Ku when short-range synapsis is blocked (Fig. 1c). Additionally, Ku depletion resulted in aberrant nuclease activity on blunt ends, 3'-overhang ends lacking microhomology, and 5'-overhang ends with internal microhomology (Fig. S10d-f). We conclude that, prior to short-range synapsis, Ku protects DNA ends from processing by both NHEJ and off-pathway enzymes, and ends become accessible for processing upon short-range synapsis. Downstream interactors

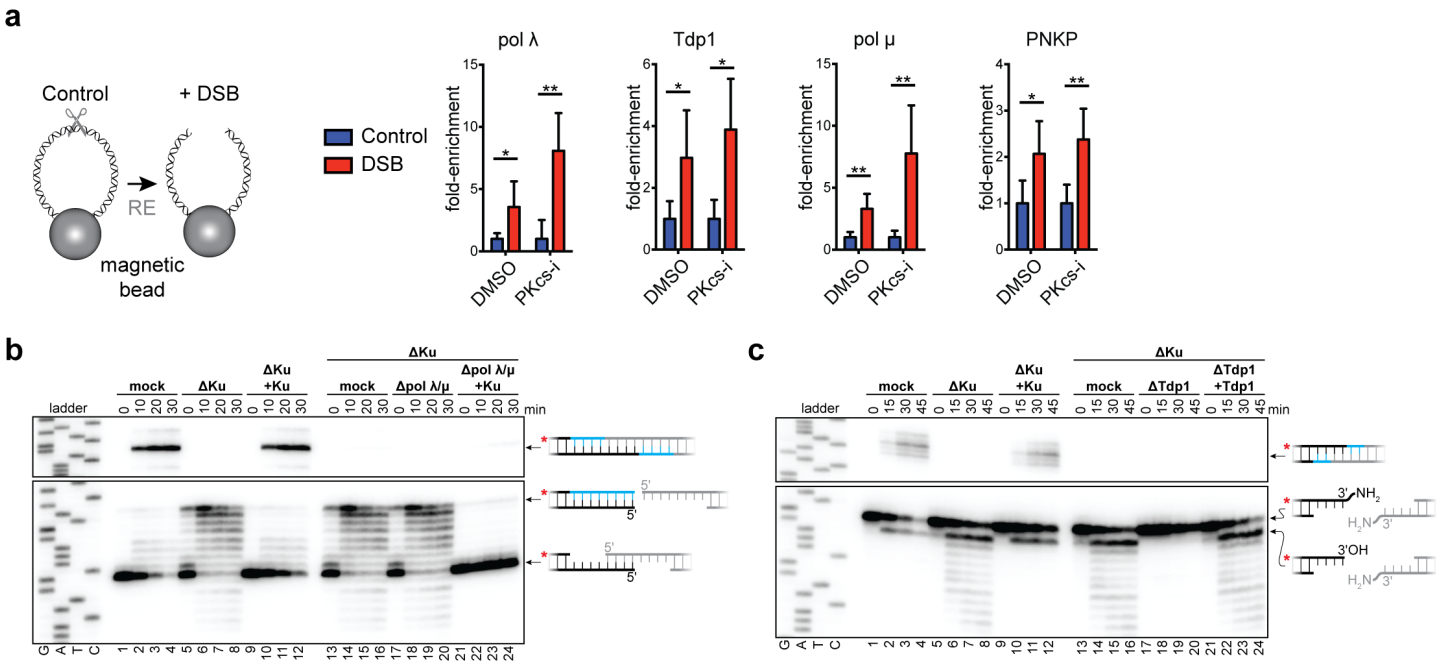

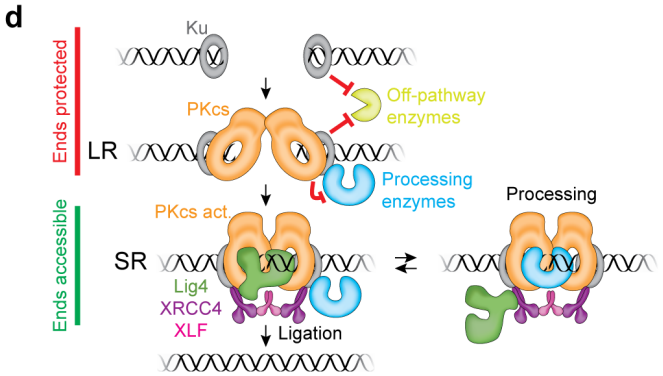

Figure 4: Ku protects DNA ends from premature and off-pathway processing. **a**, Western blot analysis of end-processing enzyme recruitment to a DSB (blunt ends introduced by XmnI digestion) in mock-treated or DNA-PKcs-inhibited extracts (see Fig. S9 for a representative experiment and explanation of quantification). Fold-enrichment is relative to undigested DNA (n = 6, mean ± s.d., *p < 0.001, **p < 0.001, two-tailed t-test). **b**,**c**, Denaturing PAGE analysis of end processing and joining of the depicted DNA ends in the indicated extracts as in Fig. 1b,c. In **b**, addition of recombinant Ku to the Ku / pol λ / pol μ-depleted extract did not rescue gap-filling and joining (lanes 21-24), indicating that pol λ was functionally depleted in this experiment. Recombinant Ku and Tdp1 were added as indicated to final concentrations of 300 nM and 40 nM, respectively. **d**, Model of DNA end processing during NHEJ. We speculate that within the short-range complex, Lig4 dynamically releases and re-engages DNA ends to allow end processing. In this scenario, a complex of XLF and XRCC4-Lig4 may maintain short-range synapsis when Lig4 is disengaged from DNA ends[28]. LR, long range complex. SR, short-range complex.

such as DNA-PKcs may also play a role in end protection, as previously reported[38,39].

As shown above, Tdp1 had measurable activity outside of the short-range synaptic complex (Fig. 3c; Fig. S7b). We postulated that Tdp1 acts on DNA ends if they are transiently unprotected prior to short-range synapsis. Consistent with this idea and the above ensemble experiments (Fig. 4c), Ku immunodepletion in the single-molecule Tdp1 assay (Fig. 3a) resulted in rapid donor loss from the low-FRET state (Fig. 3e, red dashed; Fig. S7c, red), and donor loss was suppressed by addition of recombinant Ku (Fig. S7c, yellow). Tdp1 has known roles outside NHEJ and does not typically alter DNA sequence[40]. These traits may explain the less stringent coupling of Tdp1 activity to the formation of the short-range synaptic complex.

Our results establish a new, comprehensive model to explain how NHEJ minimizes mutagenesis while efficiently repairing incompatible DNA ends (Figure 4d). Ends are initially protected from unrestricted processing by Ku, whereafter short-range synaptic complex formation stimulates end processing. Confining processing events to the short-range complex minimizes mutagenesis in multiple ways. First, because Lig4 is required for short-range synapsis, compatible DNA ends have a high probability to undergo ligation without processing, as seen in extracts (Fig. S1, #1-3) and in cells[6]. Second, as soon as incompatible ends become compatible, they undergo ligation, avoiding unnecessary processing (Fig. S1). Finally, short-range synapsis promotes utilization of pre-existing microhomology (Fig. S1, #4-5). This feature should help preserve the original sequence in cases where DSBs retain base complementarity but have damaged, unligatable termini, such as 3'-phosphoglycolates introduced by ionizing radiation[41]. Consistent with our new model, NHEJ polymerase activity in human cell extracts requires Lig4-XRCC4[21,42,43], XLF[44], and DNA-PKcs kinase activity[43]. Our results also provide evidence that end-processing enzymes are employed hierarchically to favor conservative modifications over sequence-altering ones (Fig. S11)[5,6]. For example, ends requiring only 5' phosphorylation are processed solely by PNKP and not polymerases or nucleases (Fig. S2d). Thus, enzymatic processing of DNA ends is finely tuned to minimize errors during DSB repair via NHEJ. Notably, our results have important implications for genome engineering. Efforts to improve the efficiency of CRISPR-Cas9-mediated gene disruption by overexpressing DSB processing enzymes[45] have been only modestly effective, most likely because such an approach does not circumvent DNA end

protection before short-range synapsis or immediate ligation of compatible ends upon short-range synapsis. Our model predicts that a more effective approach would be to increase DNA end accessibility prior to ligation, thereby facilitating activity of processing enzymes.

Supplemental information

Supplemental information includes figures, materials and methods, and sequencing data analysis and can be found online.

Author contributions

B.M.S. performed all experiments, with the exception of DNA pull-down experiments, which were performed by A.T.M. J.J.L., J.C.W., and B.M.S. designed experiments, analyzed the data, and wrote the paper with input from A.T.M.

Competing interests

The authors declare no competing interests.

Acknowledgments

We thank R. Scully, T. Graham, I. Rivera, and members of the Walter and Loparo laboratories for helpful discussions and comments on the manuscript. This work was supported by National Institutes of Health grant R01GM115487 (to J.J.L.) and The Howard Hughes Medical Institute (to J.C.W.). B.M.S. is supported by a postdoctoral fellowship from the Damon Runyon Cancer Research Foundation. J.C.W. is an investigator of the Howard Hughes Medical Institute.

References

1. Karanam, K., Kafri, R., Loewer, A. & Lahav, G. Quantitative Live Cell Imaging Reveals a Gradual Shift between DNA Repair Mechanisms and a Maximal Use of HR in Mid S Phase. Mol Cell 47, 320–9 (2012).
2. Radhakrishnan, S., Jette, N. & Lees-Miller, S. P. Non-homologous end joining: Emerging themes and unanswered questions. DNA Repair 17, 2–8 (2014).
3. Lieber, M. R. The Mechanism of Double-Strand DNA Break Repair by the Nonhomologous DNA End-Joining Pathway. Annu Rev Biochem 79, 181–211 (2010).
4. Chiruvella, K. K., Liang, Z. & Wilson, T. E. Repair of Double-Strand Breaks by End Joining. Cold Spring Harb Perspect Biol 5, a012757 (2013).
5. Waters, C. A., Strande, N. T., Wyatt, D. W., Pryor, J. M. & Ramsden, D. A. Nonhomologous end joining: A good solution for bad ends. DNA Repair 17, 39–51 (2014).
6. Waters, C. A. et al. The fidelity of the ligation step determines how ends are resolved during nonhomologous end joining. Nat Commun 5, 4286 (2014).
7. Graham, T., Walter, J. C. & Loparo, J. J. Two-Stage Synapsis of DNA Ends during Non-homologous End Joining. Mol Cell 61, 850–858 (2016).
8. Walker, J. R., Corpina, R. A. & Goldberg, J. Structure of the Ku heterodimer bound to DNA and its implications for double-strand break repair. Nature 412, 607 (2001).
9. Mimori, T., Hardin, J. & Steitz, J. Characterization of the DNA-binding protein antigen Ku recognized by autoantibodies from patients with rheumatic disorders. J Biological Chem 261, 2274–8 (1986).
10. Falck, J., Coates, J. & Jackson, S. P. Conserved modes of recruitment of ATM, ATR and DNA-PKcs to sites of DNA damage. Nature 434, 605 (2005).
11. Kurimasa, A. et al. Requirement for the Kinase Activity of Human DNA-Dependent Protein Kinase Catalytic Subunit in DNA Strand Break Rejoining. Mol Cell Biol 19, 3877–3884 (1999).
12. Kienker, L. J., Shin, E. & Meek, K. Both V(D)J recombination and radioresistance require DNA-PK kinase activity, though minimal levels suffice for V(D)J recombination. Nucleic Acids Res 28, 2752–2761 (2000).
13. Meek, K., Dang, V. & Lees-Miller, S. P. DNA-PK: The Means toJustify the Ends? Advances in immunology 99, 33–58 (2008).
14. Chen, L., Trujillo, K., Sung, P. & Tomkinson, A. E. Interactions of the DNA Ligase IV-XRCC4 Complex with DNA Ends and the DNA-dependent Protein Kinase. J Biol Chem 275, 26196–26205 (2000).
15. Grawunder, U. et al. Activity of DNA ligase IV stimulated by complex formation with XRCC4 protein in mammalian cells. Nature 388, 492–495 (1997).
16. Ahnesorg, P., Smith, P. & Jackson, S. P. XLF Interacts with the XRCC4-DNA Ligase IV Complex to Promote DNA Nonhomologous End-Joining. Cell 124, 301–313 (2006).
17. Bertocci, B., Smet, A., Weill, J.-C. & Reynaud, C.-A. Nonoverlapping Functions of DNA Polymerases Mu, Lambda, and Terminal Deoxynucleotidyltransferase during Immunoglobulin V(D)J Recombination In Vivo. Immunity 25, 31–41 (2006).
18. Bertocci, B., Smet, A., Berek, C., Weill, J.-C. & Reynaud, C.-A. Immunoglobulin κ Light Chain Gene Rearrangement Is Impaired in Mice Deficient for DNA Polymerase Mu. Immunity 19, 203–211 (2003).
19. Ma, Y. et al. A Biochemically Defined System for Mammalian Nonhomologous DNA End Joining. Mol Cell 16, 701–713 (2004).
20. Mahajan, K. N., McElhinny, S. A., Mitchell, B. S. & Ramsden, D. A. Association of DNA Polymerase μ (pol μ) with Ku and Ligase IV: Role for pol μ in End-Joining Double-Strand Break Repair. Mol Cell Biol 22, 5194–5202 (2002).
21. Lee, J. et al. Implication of DNA Polymerase λ in Alignment-based Gap Filling for Nonhomologous DNA End Joining in Human Nuclear Extracts. J Biol Chem 279, 805–811 (2004).

22. Ma, Y., Pannicke, U., Schwarz, K. & Lieber, M. R. Hairpin Opening and Overhang Processing by an Artemis/DNA-Dependent Protein Kinase Complex in Nonhomologous End Joining and V(D)J Recombination. Cell 108, 781–794 (2002).
23. Koch, C. et al. Xrcc4 physically links DNA end processing by polynucleotide kinase to DNA ligation by DNA ligase IV. EMBO J 23, 3874–3885 (2004).
24. Inamdar, K. V. et al. Conversion of Phosphoglycolate to Phosphate Termini on 3′ Overhangs of DNA Double Strand Breaks by the Human Tyrosyl-DNA Phosphodiesterase hTdp1. J Biol Chem 277, 27162–27168 (2002).
25. Interthal, H., Chen, H. & Champoux, J. J. Human Tdp1 Cleaves a Broad Spectrum of Substrates, Including Phosphoamide Linkages. J Biol Chem 280, 36518–36528 (2005).
26. Pannunzio, N. R., Watanabe, G. & Lieber, M. R. Nonhomologous DNA end-joining for repair of DNA double-strand breaks. J Biol Chem 293, 10512–10523 (2018).
27. Ma, Y., Lu, H., Schwarz, K. & Lieber, M. R. Repair of Double-Strand DNA Breaks by the Human Nonhomologous DNA End Joining Pathway: The Iterative Processing Model. Cell Cycle 4, 1193–1200 (2005).
28. Thode, S., Schäfer, A., Pfeiffer, P. & Vielmetter, W. A novel pathway of DNA end-to-end joining. Cell 60, 921–928 (1990).
29. Pfeiffer, P. & Vielmetter, W. Joining of nonhomologous DNA double strand breaks in vitro. Nucleic Acids Res 16, 907–924 (1988).
30. Sandoval, A. & Labhart, P. Joining of DNA ends bearing non-matching 3′-overhangs. DNA Repair 1, 397–410 (2002).
31. Graham, T. G., Carney, S. M., Walter, J. C. & Loparo, J. J. A single XLF dimer bridges DNA ends during nonhomologous end joining. Nat Struct Mol Biol 25, 877–884 (2018).
32. McElhinny, S. A. et al. A Gradient of Template Dependence Defines Distinct Biological Roles for Family X Polymerases in Nonhomologous End Joining. Mol Cell 19, 357–366 (2005).
33. Chang, H. H., Watanabe, G. & Lieber, M. R. Unifying the DNA End-processing Roles of the Artemis Nuclease: Ku-dependent Artemis Resection at Blunt DNA Ends. J Biol Chem 290, 24036–24050 (2015).
34. Chiruvella, K. K., Liang, Z., Birkeland, S. R., Basrur, V. & Wilson, T. E. Saccharomyces cerevisiae DNA Ligase IV Supports Imprecise End Joining Independently of Its Catalytic Activity. Plos Genet 9, e1003599 (2013).
35. Reid, D. A. et al. Bridging of double-stranded breaks by the nonhomologous end-joining ligation complex is modulated by DNA end chemistry. Nucleic Acids Res 45, 1872–1878 (2017).
36. Liang, F. & Jasin, M. Ku80-deficient Cells Exhibit Excess Degradation of Extrachromosomal DNA. J Biol Chem 271, 14405–14411 (1996).
37. Lee, S. et al. Saccharomyces Ku70, Mre11/Rad50, and RPA Proteins Regulate Adaptation to G2/M Arrest after DNA Damage. Cell 94, 399–409 (1998).
38. Ding, Q. et al. Autophosphorylation of the Catalytic Subunit of the DNA-Dependent Protein Kinase Is Required for Efficient End Processing during DNA Double-Strand Break Repair. Mol Cell Biol 23, 5836–5848 (2003).
39. Cui, X. et al. Autophosphorylation of DNA-Dependent Protein Kinase Regulates DNA End Processing and May Also Alter Double-Strand Break Repair Pathway Choice. Mol Cell Biol 25, 10842–10852 (2005).
40. El-Khamisy, S. F. & Caldecott, K. W. TDP1-dependent DNA single-strand break repair and neurodegeneration. Mutagenesis 21, 219–224 (2006).
41. Povirk, L. F. Processing of Damaged DNA Ends for Double-Strand Break Repair in Mammalian Cells. Isrn Mol Biology 2012, 1–16 (2012).
42. Lee, J., Yannone, S. M., Chen, D. J. & Povirk, L. F. Requirement for XRCC4 and DNA ligase IV in alignment-based gap filling for nonhomologous DNA end joining in vitro. Cancer Res 63, 22–4 (2003).
43. Budman, J., Kim, S. A. & Chu, G. Processing of DNA for Nonhomologous End-joining Is Controlled by Kinase Activity and XRCC4/Ligase IV. J Biol Chem 282, 11950–11959 (2007).
44. Tsai, C. J., Kim, S. A. & Chu, G. Cernunnos/XLF promotes the ligation of mismatched and noncohesive DNA ends. Proc National Acad Sci 104, 7851–7856 (2007).
45. Chari, R., Mali, P., Moosburner, M. & Church, G. M. Unraveling CRISPR-Cas9 genome engineering parameters via a library-on-library approach. Nat Methods 12, nmeth.3473 (2015).